Quantum beats and ultrafast solvation dynamics

B. Zolotov and D. Huppert[a)]
Raymond and Beverly Sackler Faculty of Exact Sciences, School of Chemistry, Tel Aviv University, Tel Aviv 69978, Israel

B. D. Fainberg
Center for Technological Education Holon, 52 Golomb Street, Holon 58102, Israel

(Received 5 January 1999; accepted 8 July 1999)

The beats during solvation dynamics have been studied theoretically and experimentally, using the heterodyne optical Kerr effect and pump–probe spectroscopy. We showed that the solvation process increases the beat contrast due to the hole-burning effect. Owing to the dipole activity of the intramolecular vibration responsible for the beats, a dipole–dipole coupling between the intramolecular vibration and the solvation coordinate is available. We have calculated a correlation function of the perturbation of nuclear motion during electronic transition, when such a coupling exists. Taking into account the linkage between the intramolecular vibration and the solvation coordinate yields better agreement between theory and the experimental data. We have evaluated the value of the linkage. The evaluation conforms with the values obtained by the computer fit of the experimental signals. © *1999 American Institute of Physics.* [S0021-9606(99)51337-8]

I. INTRODUCTION

Quantum beats in transient four-photon spectroscopy of nondegenerate electronic states of large molecules in condensed phase have been observed both on nonresonance[1–4] and also on resonance excitation[5–12] with pump pulses short compared with the beat period (impulsive excitation). In particular, the beats were observed on resonance excitation in pump-probe spectroscopy,[6–8,10] in transient dynamics measurements of dichroism and birefringence,[9] in transient grating spectroscopy,[6] and in three pulse stimulated photon echo experiments.[5,6] The experiments on pump–probe and transient grating spectroscopy were carried out with both very short pump pulses (pulse duration $t_p \sim 10$ fs),[6,10] and pulses long compared with electronic dephasing.[7,8]

First electron-vibrational theories of beats on resonance excitation[9,13] concerned experiments[7–9] carried out with pump pulses long compared with electronic dephasing. It has been pointed out in Ref. 13 that two mechanisms could have been responsible for the observed beats: Herzberg–Teller (non-Condon) and Franck–Condon one. The estimations of relative contributions to the beats from these mechanisms[13] and whether they originate either from the excited or the ground electronic states[9,13] have been provided by the steady-state spectra of a chromophore in a solvent. A theory of beats excited with pump pulses short compared with electronic dephasing was developed in Ref. 14.

It is worthy of note that the low frequency beats on resonance excitation with pump pulses long compared with electronic dephasing, occur on the time scale of the dynamics of electronic spectra of molecules in solutions (solvation dynamics). Therefore, the corresponding methods of spectroscopy can be considered as ''impulsive hole burning,''[15] since there are both the impulsive excitation of molecular vibrations (pulses short compared with the beat period) and hole burning (pulses long compared with electronic dephasing)[14,16–18] in these experiments.

This paper is devoted to a systematic (experimental and theoretical) study of impulsive hole burning. It is a fascinating problem because it involves two different processes: Intramolecular one (beats) and intermolecular one (solvation dynamics) occurring on the same time scale that enable us to study their mutual influence on each other. Such an influence can be as follows. First, the increase in beats contrast due to the hole-burning effect in a solvation process. The second effect is more interesting and is related to the fact that the beat frequencies for the molecules under investigation in this work are also active in their infrared spectra (see below). Therefore, we consider that a component of the dipole moment of an IR (infrared) transition $D'(z)=(\partial D/\partial z)_{z_0} z$ exists, where z denotes the vibrational coordinate corresponding to the beats. Due to the last fact, at least the dipole–dipole coupling between a vibration z and the solvation coordinate x is available. As a consequence, the beat attenuation will be related to solvation dynamics, the situation which is similar to the vibrational relaxation of a polar diatomic molecule in polar liquids.[19]

Using the heterodyne optical Kerr effect (HOKE) and pump–probe spectroscopy we observed low frequency beats (~ 150 cm^{-1}) in several polymethine dyes during the solvation process in a number of solvents. The employment of different solvents in which solvation dynamics changes from fast (methanol) to relatively slow (hexanol) enabled us to study different regimes of impulsive hole burning. We will show that the beats intensity and attenuation strongly depend on the solute. The outline of the paper is as follows. In Sec. II we describe our experiment. In Sec. III A we study the hole-burning effect in a solvation process on the beat contrast. In Sec. III B we calculate the correlation function for impulsive hole burning when the coupling between intramolecular vibration and solvation dynamics exists. Then we ap-

a)Electronic mail: huppert@chemosfl.tau.ac.il

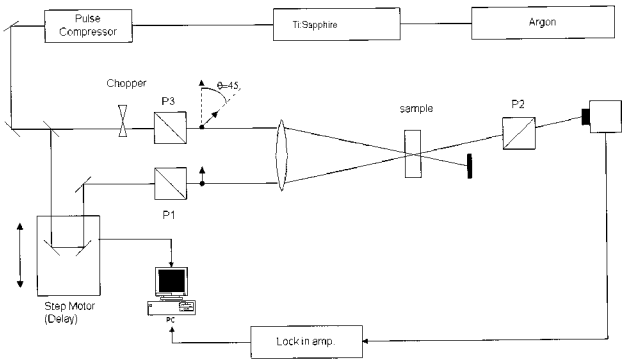

FIG. 1. Schematic diagram of the experimental apparatus; P_1, P_2 are crossed Glan–Thomson polarized pair; the polarizer P_3 is oriented at 45° with respect to P_1. The laser system consists of a CW mode locked Ti:sapphire laser pumped by a CW argon laser.

ply our results to fit of the experimental data, and evaluate the value of the coupling under consideration. In the Appendix we present relationships between the nonlinear polarization and the correlation function for impulsive hole burning.

II. EXPERIMENTAL STUDY OF "IMPULSIVE HOLE BURNING"

A. Experimental setup

The experimental system is shown in Fig. 1. A passively CW (clockwise) mode locked Ti:Sapphire laser (Coherent Mira 900F) is pumped by an Argon ion laser (Coherent Innova 310) to produce 76 MHz train of short pulses with 70–120 fs full width at half maximum (FWHM) tunable in the optical range of 720–800 nm. The laser out-put beam of 6 nJ/pulse is split into pump and probe beams with an intensity ratio of 3:1, respectively.

In the time resolved resonance HOKE experiment, the laser induced anisotropy created by the resonant absorption of the pump pulse photons is probed by a variably delayed, weak polarized probe pulse. The change in the polarization state of the probe beam is detected by the transmission through a crossed polarizer pair (P_1 and P_2 in Fig. 1) of the probe beam as a function of the time delay between the pump and the probe pulses.

In order to amplify the optical Kerr signal and to avoid complexity due to the quadratic nature of the signal, we use heterodyne methods in the signal detection. A local oscillator is derived by a small rotation of the analyzer polarizer (P_2) by $<1°$ from the maximum extinction position part of the probe pulse which is in phase, and polarized orthogonal to the probe polarization. The magnitude of the local oscillator intensity is about 30 times that of the Kerr signal. The use of a local oscillator (LO) with field $\mathcal{E}_{\mathrm{LO}}$ and light intensity I_{LO} to detect a signal with a field $\mathcal{E}_s$ and intensity I_s results in a detector response

$$I_{\mathrm{LO}}+I_s+\frac{nc}{8\pi}(\mathcal{E}_s^*\mathcal{E}_{\mathrm{LO}}+\mathcal{E}_{\mathrm{LO}}^*\mathcal{E}_s).$$

The crossed term in parenthesis is the heterodyne term.

The sample was measured in a rotating cell to avoid thermal contribution to the OKE signal. Unlike the nonresonant OKE measurement, which is used to measure the dynamics of liquids,[20] the resonance measurements provide the solvation dynamics of probe molecules in solution.

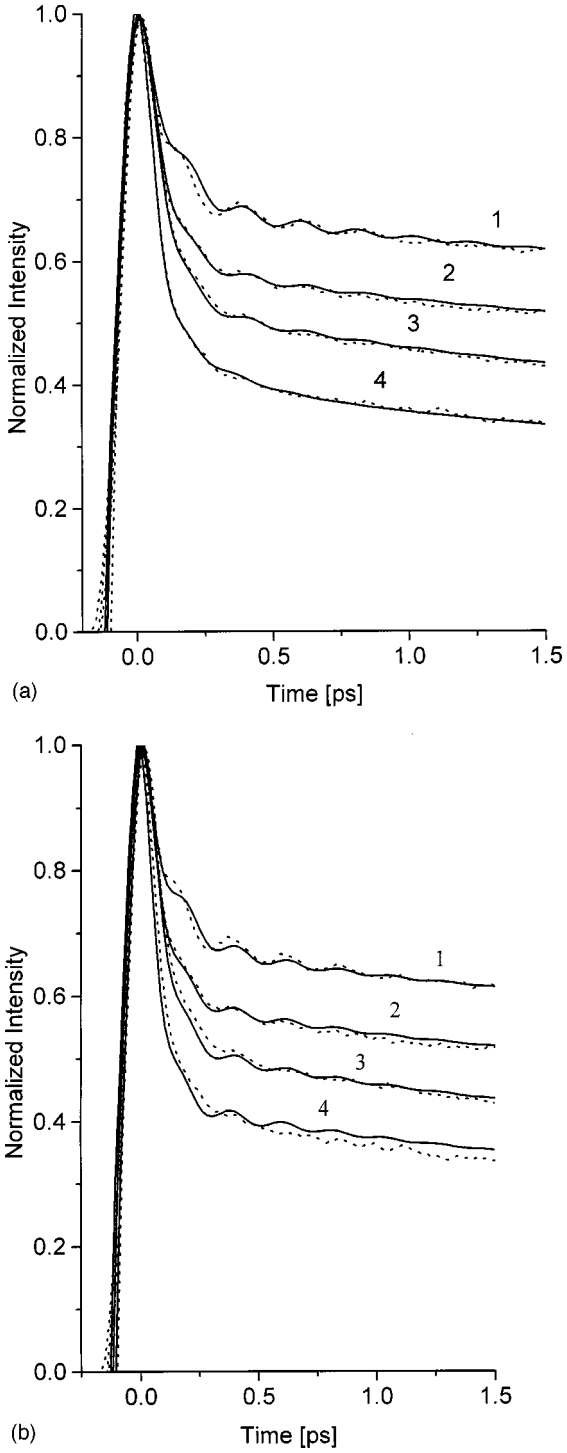

FIG. 2. The short time behavior of the HOKE signals for cryptocyanine in hexanol (1), butanol (2), ethanol (3), and methanol (4); dots—experimental results, solid lines—computer fit with (a) and without (b) taking into account the linkage between the intramolecular vibration and solvation dynamics. The parameters used to fit the data are given in Tables I–III.

B. Experimental results

Figures 2 and 3 show our experimental HOKE data concerning beats for cryptocyanine (1,1′-diethyl-4,4′carbo-

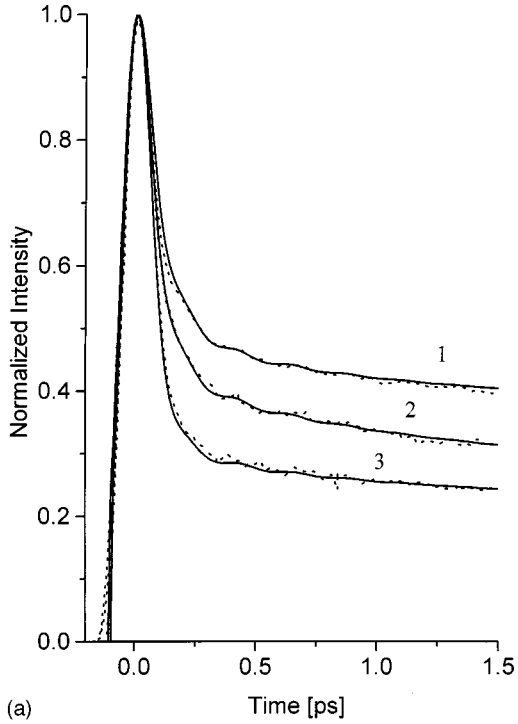

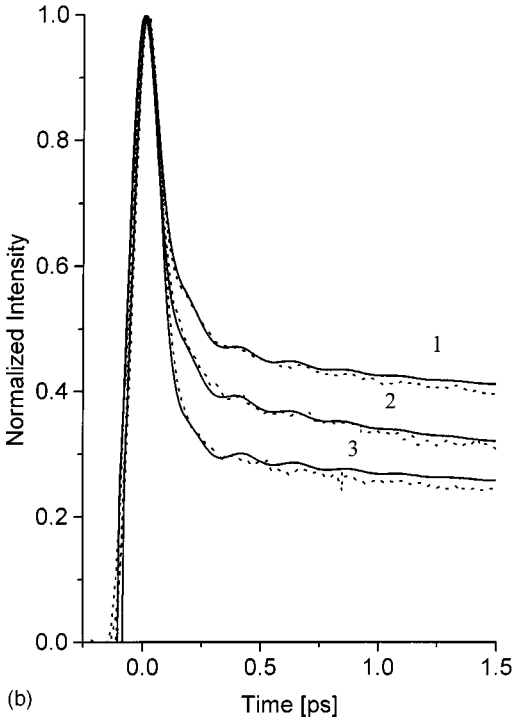

FIG. 3. The short time behavior of the HOKE signals for cryptocyanine in valeronitrile (1), butyronitrile (2), and acetonitrile (3); dots—experimental results, solid lines—computer fit with (a) and without (b) taking into account the linkage between the intramolecular vibration and solvation dynamics. The parameters used to fit the data are given in Tables I–III.

cyanine iodide) in alcohols and nitriles. We can see that the depth of the modulation of the beats is larger in the slow relaxing solvents. The beats are almost invisible in solvents with a fast relaxing Gaussian component of an appreciable amplitude like nitriles and methanol. This fact can be explained by the hole-burning effect during a solvation process (see Sec. III A).

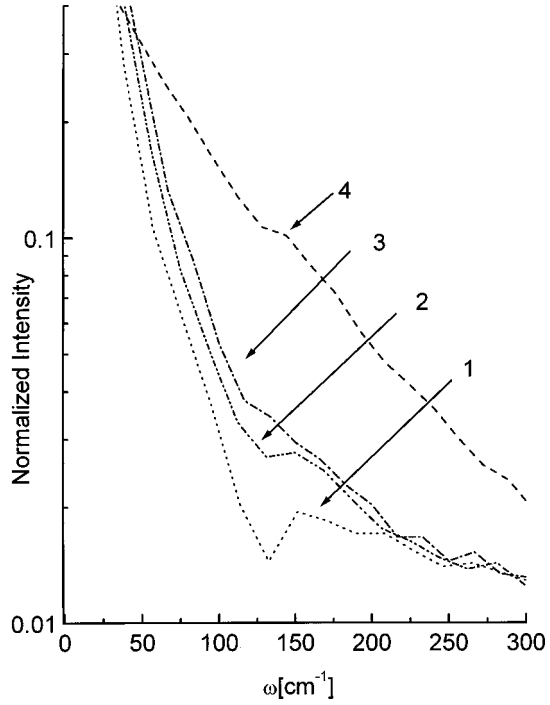

FIG. 4. The Fourier transforms of the short time behavior of the HOKE signals of cryptocyanine in hexanol (1), butanol (2), ethanol (3), and methanol (4).

Figures 4 and 5 show the Fourier-transformed experimental data into frequency domain. All the spectra display a peak near 150 cm^{-1} (including nitrile solvents).

We also observed low frequency beats for a similar molecule, 3,3′-diethylthiacarbocyanine iodide (DTTCI) for

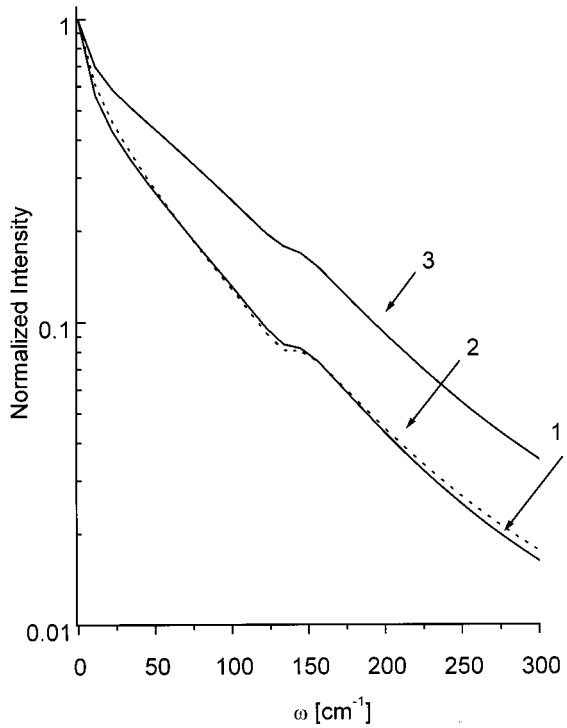

FIG. 5. The Fourier transforms of the short time behavior of the HOKE signals of cryptocyanine in valeronitrile (1), butyronitrile (2), and acetonitrile (3).

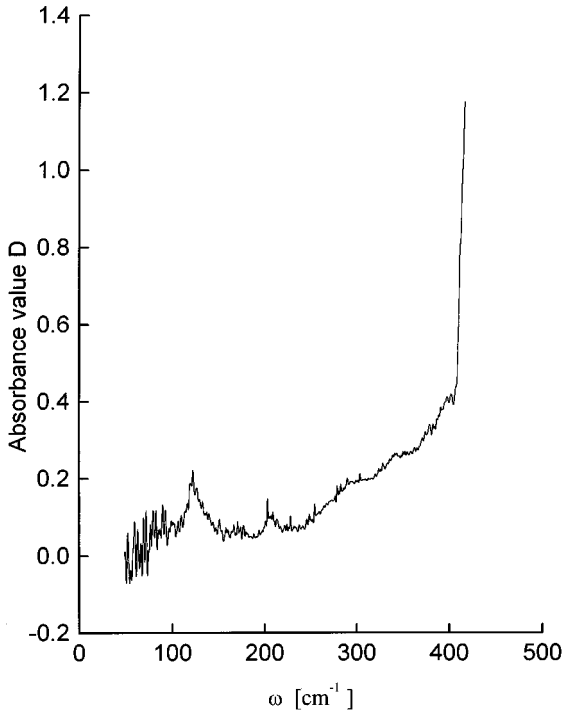

FIG. 6. The IR spectrum of DTTCI.

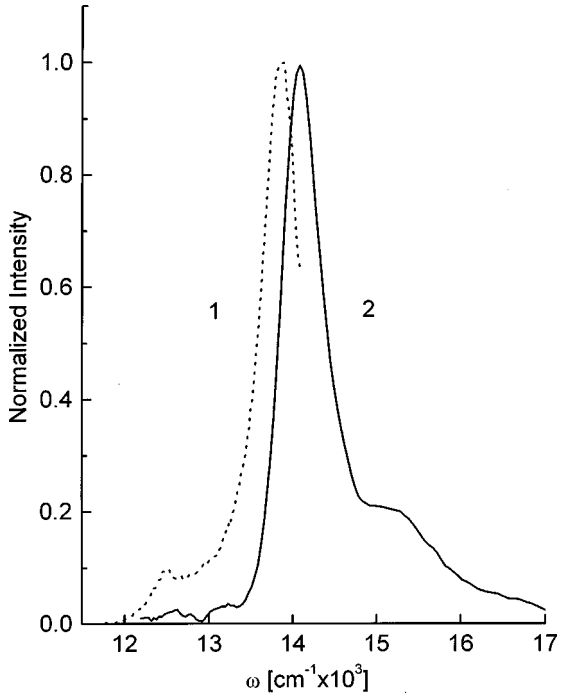

FIG. 8. Emission (1) and absorption (2) spectra of cryptocyanine in ethanol.

which the beat frequency is also active in the infrared spectrum of this molecule (see Fig. 6). Therefore, we consider that the beats under consideration correspond to a low frequency intramolecular vibrations.

Let us consider the cryptocyanine data. The cryptocyanine molecule belongs to the polymethine dyes (see Fig. 7). It consists of a conjugate system linked on both sides symmetrically to the same ring structure. Both the absorption and the emission exhibit a simple vibronic structure with a mirror symmetry (Fig. 8). Using the fitting procedure, described below, yielded a good fit of the computed signal with the experimental one. The experimental data at long times (i.e., longer than 1.5 ps) was fitted to one or two exponents (see Sec. III B 1). The excited state lifetime of cryptocyanine is relatively short. In low viscosity liquids, the excited state lifetime scales *linearly* with the solvent viscosity. The excited state lifetimes of cryptocyanine at room temperature was measured for various liquids using time correlated single photon counting technique. They are in agreement with the longest component of the OKE signals of the low viscosity liquids. In addition to the excited state lifetime, the HOKE signal consists of long time components corresponding to the diffusional solvent response which contribute to the solvation correlation function. The data of cryptocyanine in methanol and ethanol were fitted with a single exponent of 2.5 and 3.5 ps, respectively (see Table I). These values are in reasonable agreement with other measurements of different probe molecules in the same liquids using other methods.

The short time high resolution HOKE signals of cryptocyanine up to 2 ps, are shown in Fig. 2 for the linear monoalcohol solvents. The signal for hexanol comprises of a short component of 100 fs FWHM followed by several damped oscillations with ~250 fs time period. For butanol, the oscillations' amplitudes are much smaller than in hexanol solutions and the damping rate is much faster. In ethanol, the oscillations are barely observed and in methanol solutions the oscillations are not observed in the OKE signal.

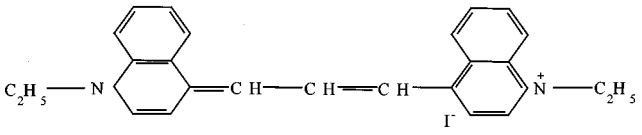

FIG. 7. The molecular structure of cryptocyanine.

III. THEORETICAL BACKGROUND

Let us consider a molecule with two electronic states $n=1$ and 2 in a solvent described by the Hamiltonian

TABLE I. Parameters of the long component of a ''pure'' solvation relaxation functions [see Eq. (24)] and the fast component amplitude $a_1=1-a_2-a_3$ for cryptocyanine in different solvents.

	$a2$	$b2$	$a3$	$b3$
	$*_{10^{12}}$ s^{-1}		$*_{10^{12}}$ s^{-1}	
MeOH	0.3	0.43	0	
EtOH	0.37	0.43	0.07	0.04
BuOH	0.35	0.43	0.18	0.04
HexOH	0.25	0.43	0.47	0.02
ACN	0.15	1.5	0	
PrCN	0.32	1	0	
BuCN	0.15	1	0.2	0.8
ValCN	0.22	1.8	0.18	0.2

$$H_0=\sum_{n=1}^{2}|n\rangle[E_n-i\hbar\gamma_n+W_n(\mathbf{Q})]\langle n|, \tag{1}$$

where $E_2>E_1$, E_n, and $2\gamma_n$ are the energy and the inverse lifetime of state n, $W_n(\mathbf{Q})$ is the adiabatic Hamiltonian of reservoir R (the vibrational subsystems of a molecule and a solvent interacting with the two-level electron system under consideration in state n).

The molecule is affected by electromagnetic radiation of three beams

$$\mathbf{E}(\mathbf{r},t)=\mathbf{E}^{+}(\mathbf{r},t)+\mathbf{E}^{-}(\mathbf{r},t)=\tfrac{1}{2}\mathbf{E}(\mathbf{r},t)\exp(-i\omega t)+c.c., \tag{2}$$

where

$$\mathbf{E}(\mathbf{r},t)=\sum_{m=1}^{3}\boldsymbol{\mathcal{E}}_m(t)\exp(i\mathbf{k}_m\mathbf{r}).$$

Since we are interested in the solvent–solute intermolecular relaxation, we shall single out the solvent contribution to $W_n(\mathbf{Q})$: $W_n(\mathbf{Q})=W_{nM}+W_{ns}$ where W_{ns} is the sum of the Hamiltonian governing the nuclear degrees of freedom of the solvent in the absence of the solute, and the part which describes interactions between the solute and the nuclear degrees of freedom of the solvent; W_{nM} is the Hamiltonian representing the nuclear degrees of freedom of the solute molecule.

A signal in any method of nonlinear spectroscopy can be expressed by the nonlinear polarization $\mathbf{P}^{NL}$.

In the transmission ''pump–probe'' experiment,[7,8,14] a second pulse (whose duration is the same as the pump pulse) probes the sample transmission ΔT at a delay τ. This dependence $\Delta T(\tau)$ is given by[21]

$$\Delta T(\tau)\sim-\omega Im\int_{-\infty}^{\infty}\mathcal{E}_{pr}^{*}(t-\tau)\mathcal{P}^{(3)+}(t)dt, \tag{3}$$

where $\mathcal{E}_{pr}$ and $\mathcal{P}^{(3)+}(t)$ are the amplitudes of the positive frequency component of the probe field and the cubic polarization, respectively.

In resonance HOKE spectroscopy[22–24] (see Sec. II A) signal can be written in the form:

$$J_{HET}\sim-Im\int_{-\infty}^{\infty}\mathcal{E}_{\mathrm{LO}}^{*}(t-\tau)\exp(i\psi)\mathcal{P}^{(3)+}(t)dt, \tag{4}$$

where ψ is the phase of the LO.

Both the absorption and the emission of the cryptocyanine molecule exhibit a simple vibronic structure with a mirror symmetry (Fig. 8). This molecule has a well structured spectra which can be considered as a progression with respect to an optically active high frequency vibration. The members of this progression are well separated, and their amplitudes rapidly attenuate when the number of the progression member increases (practically, as one can see from Fig. 8, the amplitude of the third component is rather small). Such a behavior provides evidence of a small change of the molecular nuclear configuration on an electronic excitation. In other words, the Franck–Condon electron–vibrational interactions in the cryptocyanine molecule are small.

The spectra under consideration are similar to the spectra of rhodamine 800 in a number of solvents exclusive of water and D_2O.[23] Previously we assumed that the intramolecular vibrational contribution to the line broadening of the R800 in solvents considered in Ref. 23 in the range between the electronic transition frequency ω_{el} and the first maximum is minimal. We will use such an assumption also for the cryptocyanine molecule. In our experiments the excitation frequency corresponds to this range ($\omega\simeq 13\,700\ \mathrm{cm}^{-1}$).

Therefore, one can use the model described in Ref. 23 for rhodamine 800 to calculate the nonlinear polarization (see Appendix). The latter can be expressed by the correlation function of the quantity $u=W_2(\mathbf{Q})-W_1(\mathbf{Q})$. Thus, the theoretical part of our study concerns mostly the calculation of the normalized correlation function $S(\tau)=\langle u_{\mathrm{cen}}(0)u_{\mathrm{cen}}(\tau)\rangle/\langle u_{\mathrm{cen}}^2(0)\rangle$, where $u_{\mathrm{cen}}=W_2-W_1-\langle W_2-W_1\rangle$, for impulsive hole burning and its manifestation in the pump–probe and resonance HOKE spectroscopy.

A. Influence of solvation dynamics on the beat contrast

Let us first consider the solvation influence on both the beat amplitude and phase. The total correlation function, describing both the solute-solvent interaction [solvation—the corresponding normalized correlation function is $f_{rs}(\tau)$] and the low frequency intramolecular vibration z [the normalized correlation function is $S_{zz}(\tau)$], can be represented in the form:

$$S(\tau)=f_{rs}(\tau)+\eta[S_{zz}(\tau)-f_{rs}(\tau)], \tag{5}$$

where $\eta=\omega_{st,z}/\omega_{st,x}$, $\omega_{st,x}$ is the Stokes shift determined by the intermolecular motions, $\omega_{st,z}$ is the contribution of the vibration z to the whole Stokes shift, index s denotes the solute–solvent contribution.

We assume that the parameter $\eta\ll 1$[13] due to the fact that we observe only the fundamental frequency of the vibration which is responsible for the beats. Let us consider the transmission pump–probe signal [Eq. (3)] and the HOKE signal for the LO phase $\psi=0$ [Eq. (4)]. Then using Eqs. (A2), (A5)–(A8) (see Appendix) for nonoverlapping and short pulses, we obtain for the transmission pump–probe and HOKE signals in the first order with respect to η

$$\begin{aligned}\Delta T(\tau),J_{\mathrm{HET}}(\tau)\sim&\sum_{+,-}\frac{1}{\sqrt{1-f_{rs}^2(\tau)}}\\&\times\exp\left[-\frac{(\omega-\omega_{el}\pm\omega_{st,x}/2)^2}{\sigma_{2s}}\frac{1-f_{rs}(\tau)}{1+f_{rs}(\tau)}\right]\\&\times\left\{1+(S_{zz}(\tau)-f_{rs}(\tau))\right.\\&\left.\times\left[\frac{2(\omega-\omega_{el}\pm\omega_{st,x}/2)^2}{\sigma_{2s}(1+f_{rs}(\tau))}+\frac{f_{rs}(\tau)}{1-f_{rs}^2(\tau)}\right]\eta\right\},\end{aligned} \tag{6}$$

where ω_{el} is the frequency of purely electronic transition, σ_{2s} is the central second moment of the absorption spectrum. One can directly see from Eq. (6) that the attenuation and the

phase of the beats are determined not only by the correlation function of the corresponding vibration $S_{zz}(\tau)$, but also by the solvation dynamics.

The maximum of the beats does not coincide with the maximum of the whole signal and appears later when the difference $S_{zz}(\tau)-f_{rs}(\tau)$ on the right-hand side of Eq. (6) differs from 0. Second, the factor before the curly brackets on the right-hand side of Eq. (6) describes a proportional reduction of the beat amplitude which is related to solvation dynamics. Third, the term $[(S_{zz}(\tau)-f_{rs}(\tau))f_{rs}(\tau)/(1-f_{rs}^2(\tau))]\eta$ on the right-hand side of Eq. (6) whose origin is the relaxation of the hole (or spike) value, strongly depends (diminishes) on the relaxation of the solvation correlation function $f_{rs}(\tau)$. Thus, solvation dynamics accelerates the beats attenuation. The last two factors are conditioned by the hole-burning effect (the spike and the hole evolution). Therefore, one can say that the hole-burning in a solvation process increases the beats contrast. We can expect that it is easier to observe beats in a slow relaxing solvent than in a solvent where the Gaussian component decays very fast and has a large amplitude. The last conclusions are illustrated in Figs. 2, 3, and 10.

B. Correlation function for impulsive hole burning when the coupling between intramolecular vibration and solvation dynamics exists

Let us calculate the correlation function for coupling of the intramolecular vibration with solvation dynamics. We consider the adiabatic Hamiltonians W_n of the following form:

$$\begin{aligned} W_1 &= T+\tfrac{1}{2}\Omega_x^2x^2+v(x,z)+U_{\text{bath1}}+U_{\text{bath2}}, \\ W_2 &= T+\tfrac{1}{2}\Omega_x^2(x-d_x)^2+v(x,z)-\Omega_z^2d_z(z-d_z/2) \\ &\quad +U_{\text{bath1}}+U_{\text{bath2}}, \end{aligned} \tag{7}$$

where

$$v(x,z)=\frac{1}{2}\Omega_z^2\left(z+v_z\frac{x}{\Omega_z^2}\right)^2,$$

$$U_{\text{bath1}}=\sum_i\frac{1}{2}\Omega_i^2\left(y_i+v_i\frac{x}{\Omega_i^2}\right)^2,$$

$$U_{\text{bath2}}=\sum_j\frac{1}{2}\Omega_j^2\left(q_j+v_j\frac{z}{\Omega_j^2}\right)^2.$$

Here x is the solvation coordinate, y_i are coordinates of the solvent bath interacting with the solvation coordinate, z is the coordinate of an intramolecular vibration responsible for the observed beats, q_j are coordinates of the intramolecular bath interacting with the coordinate z. We used for the potential energies of the bathes and the vibration z and their interactions with the solvation coordinate, the form proposed by Zwanzig.[25]

The correlation function of the magnitude $u_{\text{cen}}=W_2-W_1-\langle W_2-W_1\rangle$, describing optical properties of the system under consideration can be presented in the form

$$\begin{aligned} \langle u_{\text{cen}}(0)u_{\text{cen}}(t)\rangle &= \hbar[\Omega_x^2\omega_{st,x}\langle x(0)x(t)\rangle \\ &\quad +\Omega_z^2\omega_{st,z}\langle z(0)z(t)\rangle \\ &\quad +2\Omega_x\Omega_z\sqrt{\omega_{st,x}\omega_{st,z}}\,\text{sign}(d_xd_z) \\ &\quad \times\langle x(0)z(t)\rangle], \end{aligned} \tag{8}$$

where $\omega_{st,x(z)}=\hbar^{-1}\Omega_{x(z)}^2d_{x(z)}^2$ is the contribution of the motion x (z) to the Stokes shift between the equilibrium absorption and emission spectra. When deriving Eq. (8), we took into account that $\langle x\rangle=\langle z\rangle=0$. Thus, we ought to calculate three correlation functions: $\langle x(0)x(t)\rangle$, $\langle z(0)z(t)\rangle$, and $\langle x(0)z(t)\rangle$.

Let us write the classic motion equations for the system:

$$\ddot{x}+x\left(\Omega_x^2+\frac{v_z^2}{\Omega_z^2}+\sum_i\frac{v_i^2}{\Omega_i^2}\right)+\left(zv_z+\sum_i y_iv_i\right)=0, \tag{9}$$

$$\ddot{z}+z\left(\Omega_z^2+\sum_j\frac{v_j^2}{\Omega_j^2}\right)+\left(xv_z+\sum_j q_jv_j\right)=0, \tag{10}$$

$$\ddot{y}_i+\Omega_i^2y_i+xv_i=0, \tag{11}$$

$$\ddot{q}_j+\Omega_j^2q_j+zv_j=0. \tag{12}$$

The reservoir variables y_i and q_j can be eliminated from Eqs. (9) and (10) by solving Eqs. (11) and (12) relative to y_i and q_j, respectively, and substitution of the obtained solutions into Eqs. (9) and (10). We next multiply both sides of the equation obtained for z by $x(0)$ and average. As a result we arrive at the equation that connects the correlation function $\langle x(0)z(t)\rangle$ with $\langle x(0)x(t)\rangle$

$$\begin{aligned} &\frac{d^2}{dt^2}\langle x(0)z(t)\rangle+\gamma\frac{d}{dt}\langle x(0)z(t)\rangle+\Omega_z^2\langle x(0)z(t)\rangle \\ &\quad +v_z\langle x(0)x(t)\rangle=0. \end{aligned} \tag{13}$$

Here we assumed that intramolecular attenuation was a Markovian one, and could be described by a constant γ.

Next we eliminate the variable z from the equation for x, and the variable x from the equation for z. In such a manner we arrive at the Langevin equations for $x(t)$ and $z(t)$. Multiplying both sides of the last equations by $x(0)$ and $z(0)$, respectively, and averaging, we obtain the equations for the correlation functions $\langle x(0)x(t)\rangle$ and $\langle z(0)z(t)\rangle$

$$\begin{aligned} &\frac{d^2}{dt^2}\langle x(0)x(t)\rangle+\Omega_x^2\langle x(0)x(t)\rangle \\ &\quad +\int_0^t\varphi(t-t')\frac{d}{dt'}\langle x(0)x(t')\rangle dt'=0, \end{aligned} \tag{14}$$

$$\begin{aligned} &\frac{d^2}{dt^2}\langle z(0)z(t)\rangle+\left(\Omega_z^2-\frac{v_z^2}{\tilde{\Omega}_x^2}\right)\langle z(0)z(t)\rangle+\gamma\frac{d}{dt}\langle z(0)z(t)\rangle \\ &\quad +\int_0^t\frac{v_z^2}{\tilde{\Omega}_x^2}S_s(t-t')\frac{d}{dt'}\langle z(0)z(t')\rangle dt'=0, \end{aligned} \tag{15}$$

where

$$\tilde{\Omega}_x^2=\Omega_x^2+\frac{v_z^2}{\Omega_z^2}. \tag{16}$$

There are two contributions to the ''memory'' describing the attenuation of the correlation function $\langle x(0)x(t)\rangle$: $\varphi(t)=\varphi_1(t)+\varphi_2(t)$. $\varphi_1(t)=\Sigma_i(v_i^2/\Omega_i^2)\cos\Omega_i t$ is the memory for solvation process, and

$$\varphi_2(t)=\frac{v_z^2}{\Omega_z^2}S_{zzi}(t), \tag{17}$$

where

$$S_{zzi}(t)=\exp\left(-\frac{\gamma}{2}t\right)\left(\cos\omega_z t+\frac{\gamma}{2\omega_z}\sin\omega_z t\right), \tag{18}$$

is the normalized correlation function of the coordinate z with no taking into account its coupling with the coordinate x, $\omega_z=\sqrt{\Omega_z^2-(\gamma/2)^2}$. The memory in Eq. (15) $(v_z^2/\tilde{\Omega}_x^2)S_s(t)$ is determined by the normalized correlation function of the ''pure'' solvation $S_s(t)$. The latter corresponds to neglecting by the term ''zv_z,'' describing a linkage between the x and z motions on the left-hand side of Eq. (9). Correspondingly, the Laplace transform of $S_s(t)$ is determined by the following equation:

$$\overline{S_s}(p)=\frac{p+\overline{\varphi_1}(p)}{p^2+\tilde{\Omega}_x^2+p\overline{\varphi_1}(p)}, \tag{19}$$

where $\overline{\varphi_1}(p)$ is the Laplace transform of $\varphi_1(t)$.

Doing so, we obtain as a result a formula for the correlation function of the magnitude u_{cen} defined by Eq. (8)

$$\begin{aligned}\langle u_{\mathrm{cen}}(0)u_{\mathrm{cen}}(t)\rangle=\frac{\hbar}{\beta}\Bigg\{&\omega_{st,x}S_{xx}(t)+\omega_{st,z}\left(1+\frac{v_z^2}{\Omega_x^2\Omega_z^2}\right)\\&\times S_{zz}(t)-2\frac{\tilde{v}_z}{\Omega_x}\sqrt{\omega_{st,x}\omega_{st,z}}\\&\times\Bigg\{\frac{1}{\Omega_z}S_{zzi}(t)+\frac{\Omega_z}{\omega_z}\int_0^t S_{xx}(t')\\&\times\exp\left[-\frac{\gamma}{2}(t-t')\right]\sin(\omega_z(t-t'))dt'\Bigg\},\end{aligned} \tag{20}$$

TABLE II. Parameters of correlation function for ''impulsive hole burning'' for cryptocyanine in different solvents.

	v_z^2/Ω_x^2 cm^{-2}	Ω_z cm^{-1}	Ω_x cm^{-1}	λ cm^{-1}	γ cm^{-1}	$\omega_{st,x}/\omega_{st,z}$
MeOH	5744	154	93	93	24	0.9
EtOH	2636	154	82	83	24	0.9
BuOH	1251	154	80	80	24	0.9
HexOH	541	154	60	61	24	0.9
ACN	2957	149	109	109	25	0.9
PrCN	2703	149	93	93	25	0.9
BuCN	2636	149	82	83	25	0.9
ValCN	2331	149	74	75	25	0.9

TABLE III. The solvent contributions to the Stokes shift ω_{st} and the central second moment σ_{2s}, frequency of the purely electronic transition ω_{el}, and the excited state lifetime τ_f for cryptocianine in different solvents.

	ω_{st} cm^{-1}	ω_{el} cm^{-1}	σ_{2s} cm^{-2}	τ_f ps
MeOH	236	14 034	49 560	29
EtOH	230	13 967	46 538	48
BuOH	213	13 908	44 730	100
HeOH	211	13 873	44 310	154
ACN	294	14 036	57 770	22.22
PrCN	254	14 027	54 156	22.22
BuCN	254	13 975	53 760	40
ValCN	271	13 920	48 673	50

where $\tilde{v}_z=v_z\,\mathrm{sign}(d_x d_z)$, $S_{xx}(t)=\langle x(0)x(t)\rangle/\langle x^2(0)\rangle$ and $S_{zz}(t)=\langle z(0)z(t)\rangle/\langle z^2(0)\rangle$ are the normalized correlation functions of the coordinates x and z, respectively.

In the last formula Ω_x is determined by a short time behavior of a pure solvation correlation function $S_s(t)$ (Ref. 26)

$$S_s(t)=1-\frac{\Omega_x^2}{2}t^2+\cdots\approx\exp\left(-\frac{\Omega_x^2}{2}t^2\right). \tag{21}$$

$S_s(t)$ is an experimentally measurable quantity. It can be determined for example as a normalized solvation correlation function for a solute which does not show beats. The correlation function $S_{zz}(t)$ can be found by solving integro-differential equation [Eq. (15)] with a kernel $(v_z^2/\tilde{\Omega}_x^2)S_s(t-t')$, whose amplitude is determined by the quantity $v_z^2/\tilde{\Omega}_x^2$.

1. Fitting experimental results

The short time OKE signals of cryptocyanine in alcohols and nitriles were fitted by Eqs. (A2), (A3), (A5)–(A8) (see Appendix) and the correlation function calculated in Sec. III B [Eq. (20)] [see Figs. 2(a) and 3(a)]. The pulse duration was $t_p\approx 75$ fs in all experiments. We modeled a pure solvation correlation function $S_s(t)$ as consists of two components: a fast one $S_{s,f}(t)$ and a slower one $S_{s,sl}(t)$

$$S_s(t)=S_{s,f}(t)+S_{s,sl}(t). \tag{22}$$

The fast component $S_{s,f}(t)=a_1 S_{\mathrm{BO}}(t)$ is modeled by an overdamped Brownian oscillator

$$\begin{aligned}S_{\mathrm{BO}}(t)=&\frac{1}{2}\left(1+\frac{\lambda}{\sqrt{\lambda^2-\Omega_x^2}}\right)\exp[-(\lambda-\sqrt{\lambda^2-\Omega_x^2})t]\\&+\frac{1}{2}\left(1-\frac{\lambda}{\sqrt{\lambda^2-\Omega_x^2}}\right)\exp[-(\lambda+\sqrt{\lambda^2-\Omega_x^2})t].\end{aligned} \tag{23}$$

The slower component $S_{s,sl}(t)$ is modeled by one or two exponents:

$$S_{s,sl}(t)=a_2\exp(-b_2 t)+a_3\exp(-b_3 t). \tag{24}$$

The fit of the experimental data is good for all solvents. The fitting parameters are given in Tables I and II. Parameters obtained from the spectra of single-photon absorption and luminescence are listed in Table III. The fit of the ex-

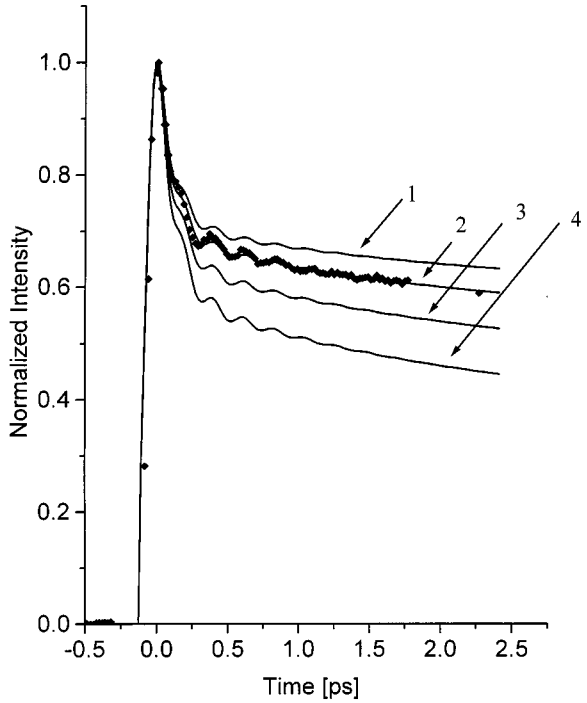

FIG. 9. Simulations of the HOKE signals for cryptocyanine in hexanol for different laser frequencies: 13 910 cm^{-1} (1), 13 710 cm^{-1} (2), 13 610 cm^{-1} (3), and 13 510 cm^{-1} (4); diamonds—experimental results. All others parameters correspond to curve 1 of Fig. 2(a).

perimental data with a correlation function (5) which does not take into account the coupling between the intramolecular vibration and solvation dynamics, yields somewhat worser results especially for fast relaxing alcohols [see Figs. 2(b) and 3(b)].

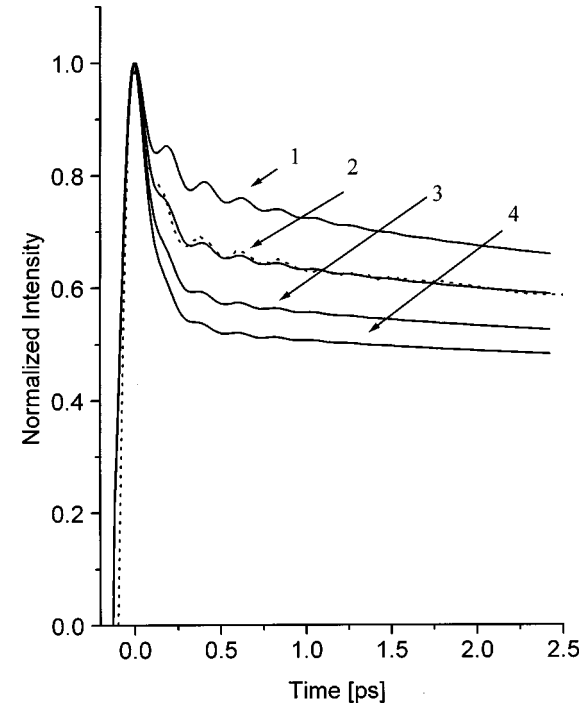

FIG. 10. Simulations of the HOKE signals with different amplitudes of the fast component: $a_1=0.1$ (1), 0.28 (2), 0.5 (3), and 0.7 (4); all others parameters correspond to curve 1 of Fig. 2(a). Dots—experimental results.

2. Effects of detuning and the amplitude of fast component

The laser frequency detuning from the electronic origin depends on the particular solvent. To study this effect on OKE signal, we carried out also the simulations of the corresponding signals for cryptocyanine in hexanol for different laser frequencies (Fig. 9). One can see that the frequency detuning affects mainly the nonmodulated part of the curves, and almost does not affect dramatically the amplitudes of the beats. In contrast, our simulations with different amplitudes of the fast component (Fig. 10) display their strong influence on the beat amplitudes. These results are in complete agreement with the conclusions of Sec. III A.

3. Evaluation of coupling between intramolecular vibration and solvation dynamics

From the fitting parameters given in Table II, it emerges that the main difference between solvents is the large difference in the value of $v_z^2/\tilde{\Omega}_x^2$, the parameter of coupling between vibration z and solvation coordinate x. Are the values obtained by the fit physically meaningful? To answer this question, we shall evaluate the value of $v_z^2/\tilde{\Omega}_x^2$. Let us denote

$$\overline{W}'_{ns}=v_z x. \tag{25}$$

Below we will show that the last quantity can be considered as the first derivative of the interaction energy between a solute and the nuclear degrees of freedom of a solvent with respect to coordinate z. In such a case the correlation function $\langle \overline{W}'_{ns}(0)\overline{W}'_{ns}(t)\rangle$ can be written in the form: $\langle \overline{W}'_{ns}(0)\overline{W}'_{ns}(t)\rangle = v_z^2\langle x(0)x(t)\rangle$, and correspondingly $v_z^2 = \langle \overline{W}'^2_{ns}(0)\rangle/\langle x^2(0)\rangle$. However, in the high-temperature (classical) approximation, the thermal average $\langle x^2(0)\rangle = 1/(\beta\Omega_x^2)$. Therefore,

$$\frac{v_z^2}{\Omega_x^2}=\beta\langle \overline{W}'^2_{ns}(0)\rangle. \tag{26}$$

Below for purposes of evaluation, we will not discriminate between $\tilde{\Omega}_x$and Ω_x.

The interaction energy between a solute in electronic state n and the nuclear degrees of freedom of a solvent is given by the formula

$$\overline{W}_{ns}(t)=-\int d\mathbf{r}\mathbf{p}(\mathbf{r})\mathbf{E}^{(n)}(\mathbf{r},z(t)),$$

where $\mathbf{p}(\mathbf{r})$ is the nuclear part of the polarization operator of the solvent (per unit volume) at point $\mathbf{r}$, $\mathbf{E}^{(n)}(\mathbf{r},z(t))$ is the electric field created by the solute molecule in electronic state n which depends on the vibrational coordinate $z(t)$. The quantity $\mathbf{E}^{(n)}(\mathbf{r},z(t))$ can be expanded with respect to the variation of the coordinate z from an equilibrium value z_0. Then

$$\overline{W}_{ns}=-\int d\mathbf{r}\mathbf{p}(\mathbf{r})\left[\mathbf{E}^{(n)}(\mathbf{r},z_0)+\left.\frac{\partial\mathbf{E}^{(n)}(\mathbf{r},z)}{\partial z}\right|_{z_0}(z-z_0)+\cdots\right]$$

$$=\overline{W}^0_{ns}+\overline{W}'_{ns}(z(t)-z_0)+\cdots, \tag{27}$$

where

$$\bar{W}'_{ns} = -\frac{\partial}{\partial z}\int d\mathbf{r}\mathbf{p}(\mathbf{r})\mathbf{E}^{(n)}(\mathbf{r},z)\big|_{z_0} \equiv -\int d\mathbf{r}\mathbf{p}(\mathbf{r})\mathbf{E}'^{(n)}(\mathbf{r},z_0). \tag{28}$$

Comparing Eqs. (27) and (28) with Hamiltonian (7), one can see that Eq. (28) for $z_0=0$ corresponds to the term $v_z x$ in the Hamiltonian (7) in accordance with Eq. (25).

Let us determine the spatial Fourier transforms of $\mathbf{p}(\mathbf{r})$ and $\mathbf{E}'^{(n)}(\mathbf{r},z_0)$

$$\mathbf{p}_\mathbf{k} = \int d\mathbf{r}\exp(i\mathbf{kr})\mathbf{p}(\mathbf{r}), \tilde{\mathbf{E}}'^{(n)}(\mathbf{k},z_0)$$

$$= \int d\mathbf{r}\exp(i\mathbf{kr})\mathbf{E}'^{(n)}(\mathbf{r},z_0). \tag{29}$$

Then we can express $\bar{W}'_{ns}$ by $\mathbf{p}_\mathbf{k}$ and $\tilde{\mathbf{E}}'^{(n)}(\mathbf{k},z_0)$

$$\bar{W}'_{ns} = -(2\pi)^{-3}\int d\mathbf{k}\mathbf{p}_\mathbf{k}\tilde{\mathbf{E}}'^{(n)}(-\mathbf{k},z_0). \tag{30}$$

Using Eq. (30), we can calculate the thermal average $\langle \bar{W}'^2_{ns}(0)\rangle$

$$\langle \bar{W}'^2_{ns}(0)\rangle = (2\pi)^{-3}\int d\mathbf{k}|\tilde{\mathbf{E}}'^{(n)}(\mathbf{k},z_0)|^2 C(\mathbf{k},0), \tag{31}$$

where $C(\mathbf{k},0)=Tr[\mathbf{p}_{-\mathbf{k}}\mathbf{p}_\mathbf{k}\exp(-\beta W_{SO})]/Tr\exp(-\beta W_{SO})$ is the amplitude of the orientational polarization correlation function of the solvent,[27,28] and W_{SO} is the Hamiltonian govering the nuclear degrees of freedom of the solvent in the absence of the solute.

Let us consider a molecule as composed from point charges at the center of each atom (or atom group). The position of each atom from the center of mass, which is assumed to be the origin, is denoted by $\mathbf{r}_i$, and its electric charge is q_i. Then the electric field created by this system of charges at the distance r from the origin can be presented in the form[29,30]

$$\mathbf{E}(\mathbf{r},\{\mathbf{r}_i\}) = \frac{1}{4\pi\varepsilon}\left[-q\nabla\left(\frac{1}{r}\right)+\mathbf{m}\nabla\nabla\left(\frac{1}{r}\right)-\cdots\right], \tag{32}$$

where $q=\Sigma_i q_i$ is the net electric charge of the molecule, $\mathbf{m}=\Sigma_i q_i\mathbf{r}_i$ is the electric moment of charges q_i relative to the origin. We introduce the electric centers of gravity of the positive and negative charges by the equations[29]

$$\sum_{pos} q_i\mathbf{r}_i = \mathbf{r}_p\sum_{pos} q_i = \mathbf{r}_p q_p$$

and

$$\sum_{neg} q_i\mathbf{r}_i = \mathbf{r}_n\sum_{neg} q_i = -\mathbf{r}_n q_n,$$

in which the radius vectors from the origin to these centers are represented by $\mathbf{r}_p$ and $\mathbf{r}_n$, and the total positive and negative charges are denoted by q_p and $-q_n$, respectively. It is clear that $q=q_p-q_n$. Then the electric moment $\mathbf{m}$ can be presented in the following form:

$$\mathbf{m}=\mathbf{D}+\Delta\mathbf{m}, \tag{33}$$

where $\mathbf{D}=(\mathbf{r}_p-\mathbf{r}_n)q_n$ is the dipole moment of the system which is independent of the choice of the origin, and $\Delta\mathbf{m}=\mathbf{r}_p q$.

The electric moment can be expanded with respect to coordinate z

$$\mathbf{m}=(\mathbf{D}_0+\Delta\mathbf{m}_0)+(\mathbf{D}'+\Delta\mathbf{m}')(z-z_0). \tag{34}$$

Then using Eqs. (28), (32), and (34), we obtain in the dipole approximation:

$$\mathbf{E}'^{(n)}_{dip}(\mathbf{r},z_0) = \frac{1}{4\pi\varepsilon}(\mathbf{D}'+\Delta\mathbf{m}')\nabla\nabla\left(\frac{1}{r}\right). \tag{35}$$

The spatial Fourier transform of this field can be found by the second formula of Eqs. (29).

Equation (35) shows that in comparison to the field of the neutral polar molecules ($\Delta\mathbf{m}'\sim q=0$), there is an additional contribution from the net charge q for molecular ions. The last effect can be a reason for different magnitudes of the parameter $v_z^2/\Omega_x^2=\beta\langle\bar{W}'^2_{ns}(0)\rangle$ [see Eq. (31)] for different alcohol solvents in our experiments. For methanol the counter ions are at a large distance from each other, and one can consider the solute molecule as a positive ion in this case. For buthanol, for example, the counter ions are at a small distance from each other, and the solute can be considered rather as a neutral molecule.

Let us evaluate the value of the parameter v_z^2/Ω_x^2. The value of the solvent contribution to the Stokes shift between the equilibrium absorption and luminescence spectra of a solute molecule in the solvent is determined by the formula[31]

$$\omega_{st} = \frac{1}{\hbar\beta}\frac{1}{(2\pi)^3}\int d\mathbf{k}|\tilde{\mathbf{E}}^{(1)}(\mathbf{k},z_0)-\tilde{\mathbf{E}}^{(2)}(\mathbf{k},z_0)|^2 C(\mathbf{k},0), \tag{36}$$

where $\tilde{\mathbf{E}}^{(1,2)}(\mathbf{k},z_0)=\int d\mathbf{r}\exp(i\mathbf{kr})\mathbf{E}^{(1,2)}(\mathbf{r},z_0)$ are the spatial Fourier transforms of fields $\mathbf{E}^{(1,2)}(\mathbf{r},z_0)$. In the dipole approximation, the magnitude of $|\tilde{\mathbf{E}}^{(1)}(\mathbf{k},z_0)-\tilde{\mathbf{E}}^{(2)}(\mathbf{k},z_0)|^2$ is proportional to $|\Delta\mathbf{D}|^2$ where $\Delta\mathbf{D}=\mathbf{D}_{11}-\mathbf{D}_{22}$ is the change of the dipole moment of a solute under electronic excitation of the solute, and $|\tilde{\mathbf{E}}'^{(n)}(\mathbf{k},z_0)|^2\sim|\mathbf{D}'|^2$. A typical value of $|\Delta\mathbf{D}|\sim|\mathbf{D}_0|\sim 1$ Debye. The magnitude of $\mathbf{D}'$ can be evaluated as $|\mathbf{D}'|^2\sim 0.01|\mathbf{D}_0|^2(2\Omega_z/\hbar)$ where $\hbar/(2\Omega_z)$ is the average value of the zero vibration amplitude squared of the vibration z. Therefore, using Eqs. (26), (31) and (36), we obtain

$$\frac{v_z^2}{\Omega_x^2}\frac{\hbar}{2\Omega_z}\Big/(\hbar\omega_{st})\sim\frac{|\mathbf{D}'|^2\hbar/(2\Omega_z)}{|\mathbf{D}_0|^2}\sim 0.01.$$

For $\Omega_z\approx 150\ \mathrm{cm}^{-1}$ and a typical value $\omega_{st}\sim 1000\ \mathrm{cm}^{-1}$, we have $v_z^2/\Omega_x^2\sim 3\cdot 10^3\ \mathrm{cm}^{-2}$ that conforms with the values obtained by the computer fit of the experimental signals (see Table II).

IV. CONCLUSIONS

In this work we have studied theoretically and experimentally the beats during solvation dynamics—impulsive hole burning.[15] We showed first that the solvation process

increases the beat contrast due to the hole-burning effect. Second, due to the dipole activity of the intramolecular vibration responsible for the beats, a dipole–dipole coupling between the intramolecular vibration and the solvation coordinate x is available. We have calculated a correlation function when such a coupling exists and have shown that in the case under consideration, the memory in Eq. (15) describing a non-Markovian attenuation of the beats, is determined by the normalized correlation function of the pure solvation $S_s(t)$. Taking into account the linkage between the intramolecular vibration and the solvation coordinate yields better agreement between theory and the experimental data.

In principle, $S_s(t)$ is an experimentally measurable quantity. It can be found from the solvation study of different solute in the same solvent. Such a procedure suggests a non-specific solvation. Unfortunately, a non-specific solvation is an ideal case and is not realized for the molecules under study. Therefore, $S_s(t)$ was fitted too.

We have evaluated the value of $v_z^2/\tilde{\Omega}_x^2$, the linkage between vibration z and solvation coordinate x. We obtained the value $\sim 3000\ \mathrm{cm}^{-2}$ that conforms with the values obtained by the computer fit of the experimental signals. This evidence is in favor of the existance of such a linkage. More experiments on this topic are in progress.

Our study shows that in comparison to the field of neutral polar molecules, there is an additional contribution from the net charge q for molecular ions [see Eq. (35)]. The last effect can be a reason for different magnitudes of the parameter v_z^2/Ω_x^2 for different alcohol solvents in our experiments. For methanol the counter ions are at a large distance from each other, and one can consider the solute molecule as a positive ion in this case. For buthanol, for example, the counter ions are at a small distance from each other, and the solute can be considered rather as a neutral molecule.

Finally we emphasize that while the $x-z$ coupling is not sharply pronounced in the quantum beat dynamics, it is very interesting, manifesting information on the correlation between intramolecular dynamics and a solvent motion.

ACKNOWLEDGMENTS

This work was supported by grants from the United States-Israel Binational Science Foundation (BSF), and the James Franck Binational German-Israel Program in Laser Matter Interaction.

APPENDIX

Let us describe the model used in Ref. 23 for rhodamine 800 in a number of solvents to calculate the nonlinear polarization. This molecule has a well structured spectra which can be considered as a progression with respect to an optically active high frequency vibration $\sim 1500\ \mathrm{cm}^{-1}$.[32] The members of this progression are well separated, and their amplitudes rapidly attenuate when the number of the progression member increases. Such a behavior provides evidence of a small change of the molecular nuclear configuration on an electronic excitation. In other words, the Franck–Condon electron–vibrational interactions in rhodamine molecules are small. The resonance Raman scattering studies of rhodamine dyes[33,34] display intense lines in the range of ~ 1200–$1600\ \mathrm{cm}^{-1}$ and the lowest-frequency one at $600\ \mathrm{cm}^{-1}$ in both alcohol and water solutions. Therefore, one can assume that the intramolecular vibrational contribution to the line broadening of the R800 in the range between the electronic transition frequency ω_{el} and the first maximum is minimal. In experiments[23] the excitation frequency corresponded to this range ($\omega = 13\,986\ \mathrm{cm}^{-1}$).

Let us discuss the interactions with the solvent. They satisfy the slow modulation limit[16–18,27,35] in the spirit of Kubo's theory of the stochastic modulation[36]

$$\tau_s^2 \sigma_{2s} \gg 1, \tag{A1}$$

where $\sqrt{\sigma_{2s}}$ plays the role of the modulation amplitude and τ_s is the characteristic time of the attenuation of the solvation correlation function.

As a consequence of condition (A1), we can obtain the following expression for the nonlinear polarization of the system[16,17]

$$\mathcal{P}^{(3)+}(t) = \frac{1}{8} \sum_{mm'm''} \int_0^\infty d\tau_2 \chi^{(3)}(\omega, t, \tau_2) \times \mathcal{E}_{m''}(t) \mathcal{E}_{m'}(t-\tau_2) \mathcal{E}_m^*(t-\tau_2), \tag{A2}$$

if the exciting pulses are Gaussian[16]

$$\mathcal{E}_m(t) = \mathcal{E}_0 \exp[-(\Delta^2/2)(t-t_m)^2 + i\omega t_m], \tag{A3}$$

with pulse duration of

$$t_p = 1.665/\Delta \gg \sigma_{2s}^{-1/2}. \tag{A4}$$

In Eq. (A2) $\chi^{(3)}(\omega, t, \tau_2)$ is the cubic susceptibility.

We consider the translational and the rotational motions of liquid molecules as nearly classical at room temperatures, since their characteristic frequencies are smaller than the thermal energy kT.

In the Condon approximation, the cubic susceptibility $\chi^{(3)}(\omega, t, \tau_2)$ can be written in the form[16]

$$\chi^{(3)}(\omega, t, \tau_2) = -i(2\pi^3)^{1/2} N L^4 \hbar^{-3} \exp(-\tau_2/T_1) \times (\sigma(\tau_2))^{-1/2} F_{0,s\alpha}^e(\omega - \omega_{el}) w(z_{\alpha,\varphi}). \tag{A5}$$

Here $F_{s\alpha}^e(\omega - \omega_{el}) = (2\pi\sigma_{2s})^{-1/2} \exp[-(\omega - \omega_{el} - \langle u_s \rangle/\hbar)^2/(2\sigma_{2s})]$ is the equilibrium absorption spectrum of a chromophore, $u_s = W_{2s} - W_{1s}$

$$w(z) = \exp(-z^2)\left[1 + (2i/\sqrt{\pi}) \int_0^z \exp(t^2) dt\right],$$

is the error function of the complex argument[37]

$$z_{\alpha,\varphi} = \{i\Delta^2[\tau_2(2 + S(\tau_2)) - t(3 + S(\tau_2)) + t_{m''} + t_{m'} + t_m(1 + S(\tau_2))] + \omega - \omega_{\alpha,\varphi}(\tau_2)\}/(2\sigma(\tau_2))^{1/2}, \tag{A6}$$

where we put $t_m = 0$ and $t_{m''} + t_{m'} = \tau$ in Eq. (A6) for the spectroscopical methods under consideration,

$$\sigma(\tau_2)=\sigma_{2s}\left\{1-S^2(\tau_2)+\frac{\Delta^2}{\sigma_{2s}}[3+2S(\tau_2)+S^2(\tau_2)]\right\}, \tag{A7}$$

is the time-dependent central second moment of the changes related to nonequilibrium processes in the absorption and the emission spectra, at the active pulse frequency ω

$$\omega_{\alpha,\varphi}(\tau_2)=\omega_{el}\pm\frac{\omega_{st}}{2}+S(\tau_2)\left[\omega-\left(\omega_{el}\pm\frac{\omega_{st}}{2}\right)\right], \tag{A8}$$

are the first moments related to the solvent contribution to transient absorption (α) and emission (φ) spectra, respectively, $\omega_{st}=2\langle u_s\rangle/\hbar$ is the solvent contribution to the Stokes shift between the equilibrium absorption and emission spectra, $\hbar^2\sigma_{2s}S(t)=\langle u_s(0)u_s(t)\rangle-\langle u_s\rangle^2$, $S(t)$ is the normalized solute–solvent correlation function, $\sigma_{2s}=\hbar^{-2}(\langle u_s^2(0)\rangle-\langle u_s\rangle^2)$ is the solvent contribution to the second central moment of both the absorption and the luminescence spectra. For the classical (high-temperature) case, σ_{2s} and ω_{st} are related by the following equation: $\sigma_{2s}=\omega_{st}\hbar^{-1}\beta^{-1}$ where $\beta=1/(kT)$. The terms $w(z_{\alpha,\varphi})$ in the right-hand side of Eq. (A5) describe the contributions to the cubic polarizations of the nonequilibrium absorption and emission processes, respectively.

The third term on the right-hand side of Eq. (A7) which is proportional to Δ^2/σ_{2s}, plays the role of the pulse width correction to the hole or spike width. This term is important immediately after the optical excitation when $\tau_2\approx 0$ and, therefore, $S(\tau_2)\approx 1$. The first term on the right-hand side of Eq. (A6) which is proportional to $\Delta^2\sim 1/t_p^2$, takes into account the contribution of the electronic transition coherence.

Bearing in mind our comments concerning the role of the intra- and intermolecular interactions, we can assume that criterion (A1) is correct for the first maxima in both the absorption and luminescence spectra of the R800. In the last case σ_{2s} is the central second moment of the first maximum.

Also the criterion (A4) is well realized in our experiments, since $t_p\sim 70$ fs and $\sigma_{2s}^{-1/2}\approx 14$ fs.

[1] Y. Yan and K. A. Nelson, J. Chem. Phys. **87**, 6240 (1987).
[2] Y. Yan and K. A. Nelson, J. Chem. Phys. **87**, 6257 (1987).
[3] S. Ruhman, A. G. Joly, and K. A. Nelson, IEEE J. Quantum Electron. **24**, 460 (1988).
[4] S. Ruhman, B. Kohler, A. G. Joly, and K. A. Nelson, IEEE J. Quantum Electron. **24**, 470 (1988).
[5] W. P. de Boeij, M. S. Pshenichnikov, and D. A. Wiersma, J. Phys. Chem. **100**, 11806 (1996).
[6] T. Joo, Y. Jia, T.-Y. Yu, M. J. Lang, and G. R. Fleming, J. Chem. Phys. **104**, 6089 (1996).
[7] M. J. Rosker, F. W. Wise, and C. L. Tang, Phys. Rev. Lett. **57**, 321 (1986).
[8] F. W. Wise, M. J. Rosker, and C. L. Tang, J. Chem. Phys. **86**, 2827 (1987).
[9] J. Chesnoy and A. Mokhtari, Phys. Rev. A **38**, 3566 (1988).
[10] H. L. Fragnito, J.-Y. Bigot, P. C. Becker, and C. V. Shank, Chem. Phys. Lett. **160**, 101 (1989).
[11] C. J. Bardeen, Q. Wang, and C. V. Shank, Phys. Rev. Lett. **75**, 3410 (1995).
[12] J. Y. Bigot, T. A. Pham, and T. Barisien, Chem. Phys. Lett. **259**, 469 (1996).
[13] B. D. Fainberg, Opt. Spectrosc. **65**, 722 (1988) [Opt. Spektrosk. **65**, 1223 (1988)].
[14] Y. J. Yan and S. Mukamel, Phys. Rev. A **41**, 6485 (1990).
[15] W. B. Bosma, Y. J. Yan, and S. Mukamel, J. Chem. Phys. **93**, 3863 (1990).
[16] B. D. Fainberg, Opt. Spectrosc. **68**, 305 (1990) [Opt. Spektrosk. **68**, 525 (1990)].
[17] B. Fainberg, Isr. J. Chem. **33**, 225 (1993).
[18] B. Fainberg, Phys. Rev. A **48**, 849 (1993).
[19] M. Cho, J. Chem. Phys. **105**, 10755 (1996).
[20] D. McMorrow and W. T. Lotshaw, J. Phys. Chem. **95**, 10395 (1991).
[21] B. D. Fainberg, Chem. Phys. **148**, 33 (1990).
[22] B. D. Fainberg, B. Zolotov, A. Gan, S. Y. Goldberg, and D. Huppert, in *Fast Elementary Processes in Chemical and Biological Systems*, edited by A. Tramer (AIP Press, Woodbury, New York, 1996), AIP Proceedings, Vol. 364, p. 454.
[23] B. Zolotov, A. Gan, B. D. Fainberg, and D. Huppert, Chem. Phys. Lett. **265**, 418 (1997).
[24] B. Zolotov, A. Gan, B. D. Fainberg, and D. Huppert, J. Lumin. **72–74**, 842 (1997).
[25] R. Zwanzig, J. Stat. Phys. **9**, 215 (1973).
[26] B. D. Fainberg and D. Huppert, Nonlinear Opt. **11**, 329 (1995); **16**, 93 (1996).
[27] R. F. Loring, Y. J. Yan, and S. Mukamel, J. Chem. Phys. **87**, 5840 (1987).
[28] B. D. Fainberg and D. Huppert, J. Mol. Liq. **64**, 123 (1995); **68**, 281 (1996).
[29] C. J. F. Böttcher, *Theory of Electric Polarization* (Elsevier Scientific Publishing Company, Amsterdam, 1973), Vol. 1.
[30] J. D. Jackson, *Classical Electrodynamics* (Wiley, New York, 1975).
[31] S. Mukamel, *Principles of Nonlinear Optical Spectroscopy* (Oxford University Press, New York, 1995).
[32] B. D. Fainberg and B. S. Neporent, Opt. Spectrosc. **48**, 393 (1980) [Opt. Spektrosk. **48**, 712 (1980)].
[33] R. B. Andreev, Y. S. Bobovich, A. V. Bortkevich, V. D. Volosov, and M. Ya. Tsenter, J. Appl. Spectrosc. **25**, 1013 (1976) [Zhurn. Prikl. Spektr. **25**, 294 (1976)].
[34] R. B. Andreev, Y. S. Bobovich, A. V. Bortkevich, V. D. Volosov, and M. Ya. Tsenter, Opt. Spectrosc. **41**, 462 (1976) [Opt. Spektrosk. **41**, 782 (1976)].
[35] B. Fainberg, R. Richert, S. Y. Goldberg, and D. Huppert, J. Lumin. **60–61**, 709 (1994).
[36] R. Kubo, in *Relaxation, Fluctuation and Resonance in Magnetic Systems*, edited by D. der Haar (Oliver Boyd, Edinburgh, 1962), p. 23.
[37] M. Abramovitz and I. Stegun, *Handbook on Mathematical Functions* (Dover, New York, 1964).